

# A Generalized Kelvin Solution Based BEM for Contact Problems of Elastic Indenter on Functionally Graded Materials

H. T. Xiao<sup>1</sup> and Z. Q. Yue<sup>2</sup>

**Abstract:** This paper presents a three-dimensional boundary element method for contact problems of an elastic indenter on the surface of functionally graded materials (FGMs). The FGM elastic properties can have any irregular variations with depth. The indenter is subjected to the loading normal to the flat contact surface. The classical Kelvin solution is used for the mathematical formulation of the homogeneous elastic indenter. The generalized Kelvin solution is used for the mathematical formulation of the FGM base. The contact variables are defined with respect to each of the surfaces using local coordinate systems. The corresponding contact equations are used to couple the two sets of the linear equation systems for the indenter and the FGM. The numerical verifications illustrate that the proposed method can obtain accurate results for the contact displacement and stress. Numerical results for an elastic rectangular plate centrally or eccentrically indenting a FGM of actual depth variation property are presented and analyzed.

**Keywords:** functionally graded materials, FGM, contact problem, BEM, elastic indenter, rigid indenter, frictional contact surface

## 1 Introduction

Functionally graded materials (FGMs) are one of the peculiar heterogeneous solid materials because their properties vary along the depth direction only and have no change along the lateral directions. Topics concerning the contact problems between an indenter and a FGM are of interest to researchers and engineers in applied mechanics and many branches of engineering.

Publications on contact problems are extensively available in the literature. A thor-

---

<sup>1</sup> Shandong Key Laboratory of Civil Engineering Disaster Prevention and Mitigation, Shandong University of Science and Technology, Qingdao, 266510, China

<sup>2</sup> Department of Civil Engineering, The University of Hong Kong, Hong Kong, China. Corresponding Author. Tel: 852-28591967; Fax: 852-25595337; Email: yueqzq@hkucc.hku.hk

ough description and review of the contact problems may be found in the treatises written by Gladwell (1980), Johnson (1985), Hills et al. (1993) and Selvadurai (2007). Some important contributions to the FGM contact problems are specially discussed below. Selvadurai (1979) and Gladwell (1980) developed the approaches to the formulation of elastostatic contact problems and embedded anchor problems dealing with isotropic and inhomogeneous elastic media. Rowe and Booker (1981) examined the axisymmetric surface settlement of a non-homogeneous elastic soil with a crust subjected to a rigid circular footing using a finite layer analysis method. Booker et al. (1985) provided analytical solutions for the behavior of a smooth rigid disc due to a normal load or a moment on the surface of a non-homogeneous half-space. Rajapakse and Selvadurai (1991) used a variational technique and further examined the axisymmetric response of a circular footing and an anchor plate in a linearly non-homogeneous elastic soil of halfspace extent. Yue and Selvadurai (1995) solved the problems of both asymmetric and axisymmetric indentation of a rigid circular plate on a saturated poroelastic halfspace. Selvadurai (1996) examined the axisymmetric indentation of a half-space by a rigid circular foundation with a smooth flat base where the shear modulus varies with depth in exponential function and the Poisson's ratio always has no change.

In more recent years, Guler and Erdogan (2006) analyzed the two-dimensional contact problems of two deformable elastic solids with graded coatings. Vignjevic et al. (2006) and Oishi et al. (2008) developed some algorithms for different contact problems. Pak et al. (2008) analyzed tensionless contact of a flexible plate and annulus with a smooth half-space with integral equation method.

In examining the FGM contact problems with analytical methods, it is generally assumed that the FGM elastic properties vary with depth in simple functions. However, such simplified depth variation models sometimes cannot represent the actual property variations in depth. Numerical methods have to be used. For example, Pender et al. (2001) used finite element method (FEM) to investigate the contact problems of a rigid indenter on a graded substrate with irregular property change in depth.

On the other hand, the use of BEM to examine contact problems has been well reported in the literature. For examples, Man et al. (1992) presented a 2D BEM analysis of contact problems with an iterative and fully-incremental technique. Olukoko et al. (1994) reviewed three alternative BEMs to model contact problems with frictional slipping. The first method is based on node-on-node matching along the interface. The other two are along an independent discretization of the contacting bodies. Hack and Backer (1999) analyzed the 2D frictional contact problems under tangential loading using the local coordinates. Leahy and Becker (1999a, 1999b) developed the 3D BEM for contact problems with frictional slipping. Gun (2004)

used the 3D BEM developed to analyze 3D elasto-plastic contact problems. Keppas et al. (2008) developed a BEM to treat 2D time dependent thermo-elastic contact problems and incorporated the thermal resistance along the contacting surfaces. Blázquez and París (2009) showed that the use of a non-conforming algorithm associated with a weak application of the contact conditions could reduce the incompatibilities and produce a smooth distribution of the contact stresses. However, the literature review of the present study indicated that there are few publications in the open literature on BEM based analysis for the FGM contact problems.

In this paper, a boundary element method (BEM) is presented for further analysis of the contact problems between an elastic indenter and a FGM, as shown in Fig. 1. The indenter is modeled as a homogeneous elastic solid and is analyzed with the conventional Kelvin solution based BEM. The FGM is modeled as a layered elastic system and analyzed with the generalized Kelvin solution based BEM (Yue, 1995; Yue and Xiao, 2002; Xiao et al. 2005). The node-on-node approach is utilized for the contact area. The contact variables are defined with respect to each surface of two domains using the local coordinate systems. The elastic indenter can be rigid if its modulus is provided with a large value. Two verifications are also presented to compare the present contact stress results with those given in the literature. The proposed BEM is further used to analyze the eccentric indentation of a rectangular elastic plate on a FGM. The FGM is the Silicon Nitride-Oxynitride Glass system given in Pender et al. (2001). Two cases of contact problems are considered. The displacements and stresses in FGM are further presented and analyzed.

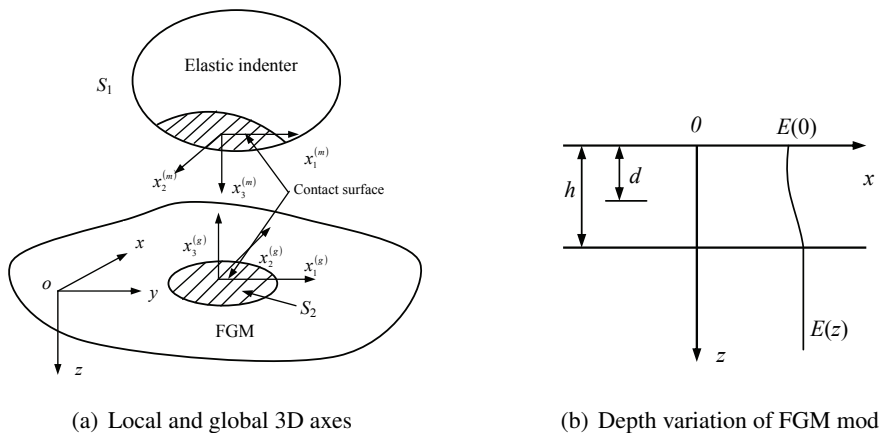


Figure 1: Contact problem between an elastic indenter and a FGM halfspace

## 2 BEM Formulations for FGM Contact Problems

### 2.1 Formulations for indenter

The indenter is modeled as a homogeneous, isotropic elastic solid. The classical Kelvin solution for a point load in a homogeneous elastic space is used for analysis of the elastic indenter shown in Fig. 1a. The boundary integral equation can be written as follows:

$$C_{ij}(P)u_j(P) = \int_{S_1} u_{ij}^K(P, Q)t_j(Q)dS(Q) - \int_{S_1} t_{ij}^K(P, Q)u_j(Q)dS(Q) \quad (1)$$

where  $u_j$  and  $t_j$  are, respectively, the displacements and tractions on the boundary surface of the indenter  $S_1$ ;  $u_{ij}^K$  and  $t_{ij}^K$  are the displacements and tractions of the Kelvin solutions;  $P$  and  $Q$  denote, respectively, the source and field points on the boundary  $S_1$ ; and  $C_{ij}(P)$  is a coefficient dependent on the local boundary geometry at the source point  $P$ .

### 2.2 Formulations for FGM

The FGM has its isotropic elastic properties variable in depth, shown in Fig. 1b. The generalized Kelvin solution given by Yue (1995) is used. This basic solution is an extension of the classical Kelvin solution and is for stress and displacement field in a layered elastic solid of infinite extent due to the action of point loads. Each layer is a homogeneous elastic solid of finite thickness and infinite lateral extension. The total number of the dissimilar elastic layers is an arbitrary integer  $n$  ( $0 \leq n < \infty$ ). The layers adhere to the first homogeneous elastic solid of upper semi-infinite extent and the last homogeneous elastic solid of lower semi-infinite extent. The interface between any two connected dissimilar layers is planar and fully bonded. All the layer interfaces are parallel to each other. The convergence and accuracy of the solution are rigorously and analytically verified. This solution has been used for the analysis of crack problems in FGMs (Yue and Xiao, 2002, Xiao et al. 2005).

For this FGM contact problem, the shear modulus of the first solid of upper semi-infinite extent is assigned a zero value (or an infinitesimal value, e.g.,  $10^{-15}$  MPa). Consequently, the first elastic solid becomes a void space of upper semi-infinite extent. The generalized Kelvin solution for a point load in a multilayered elastic solid of infinite extent is automatically degenerated into the generalized Boussinesq-Cerruti solution for a point load in a layered halfspace (Yue, et al. 1999).

For  $0 \leq z \leq h$ , the FGM is modeled as the layered elastic solid. Each layer has the thickness equal to  $h/n$ . Each layer has its elastic modulus  $E(z)$  and Poisson ratio

$v(z)$  at its upper depth. For  $h \leq z < \infty$ , the FGM is modeled as the last homogeneous elastic solid of lower semi-infinite extent. If its shear modulus approaches to infinity or is assigned an extremely large value (say,  $10^{15}$  MPa), this last elastic solid would become a rigid base foundation to support the above FGM layer.

As Yue and Xiao (2002) and Xiao et al. (2005), a large layer number  $n$  is selected for obtaining the solution of the FGM with a good degree of accuracy.

The displacements on the FGM contact surface can be expressed as

$$u_i(Q) = \int_{S_2} u_{ij}^Y(Q, P) t_j(P) dS(P) \quad (2)$$

where  $u_{ij}^Y$  is the displacements of the generalized Kelvin solution;  $S_2$  is the contact surface;  $P$  and  $Q$  denote, respectively, the source and field points on the boundary  $S_2$ .

It is noted that Eq. 2 does not contain the integration on the layer interfaces because the solution strictly satisfies the interface conditions. Discretization along layer interfaces are not needed in this BEM formulation. Thus, similar to Mindlin solution based BEM, only the contact surface is needed to be discretized.

Eqs. 1 and 2 are discretized accordingly. The eight-noded isoparametric elements are employed to discretize the indenter surface and the contact face (Fig.2). Two sets of linear equation system are obtained for solution of the unknown contact displacements and contact stresses. For a rigid indenter, the contact stresses are singular at the contact circumference (Yue, 1996). In order to accurately compute the displacements and stresses near the contact circumference, the traction singular elements of eight nodes are used (Xiao et al. 2005).

### 2.3 Contact conditions

When the elastic indenter contacts the FGM, each solid has a normal direction  $x_3$  and two orthogonal tangential directions  $x_1$  and  $x_2$ , as shown in Fig. 1a. The coordinate systems in Fig. 1a follow the right-hand side screw rule. Each contact node has six contact variables which are the three contact displacements and the three contact stresses.

The contact conditions are the continuity of the two normal displacements and the equilibrium condition for each pair of the six contact stresses. They are imposed on the contact node pairs.

In addition, two contact cases are considered. The first case is that the contact is fully bonded, where the two contact tangential displacements along each of the two orthogonal tangential directions are equal. The second case is that the contact has

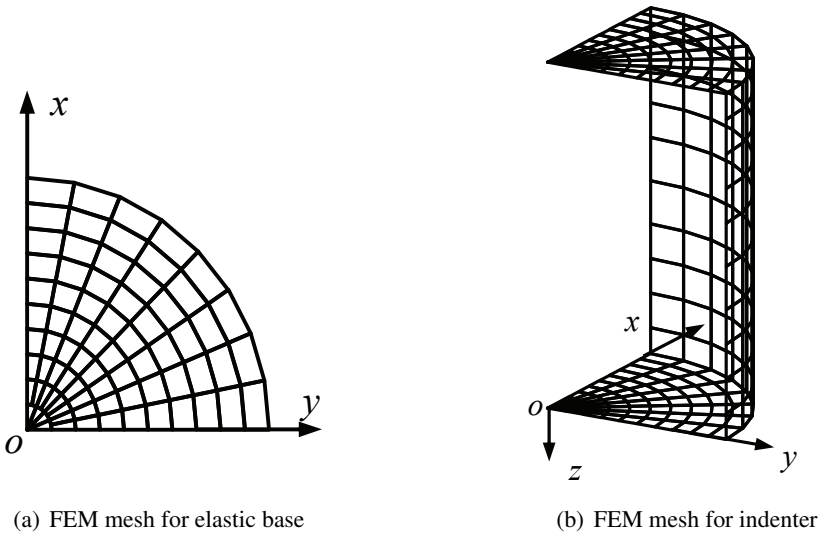


Figure 2: Axisymmetric FEM meshes for indentation of an elastic circular cylinder on a homogeneous elastic base of half space extent

frictional slippage that follows the Coulomb frictional criterion, where the two contact tangential displacements along each of the two orthogonal tangential directions are different.

Let the symbol  $(m)$  for the indenter and the symbol  $(g)$  for the FGM. In the local coordinate systems, the common contact conditions for the two cases at a node pair can be expressed as follows:

$$u_{x_3}^{(m)} = -u_{x_3}^{(g)} + \delta \quad (3)$$

$$t_{x_3}^{(m)} = t_{x_3}^{(g)} \quad (4)$$

$$t_{x_1}^{(m)} = -t_{x_1}^{(g)} \quad (5)$$

$$t_{x_2}^{(m)} = t_{x_2}^{(g)} \quad (6)$$

The additional contact conditions for the first case at a node pair can be expressed as follows:

$$u_{x_1}^{(m)} = u_{x_1}^{(g)} \quad (7)$$

$$u_{x_2}^{(m)} = -u_{x_2}^{(g)} \quad (8)$$

The additional contact conditions for the second case at a node pair can be expressed as follows:

$$t_{x_1}^{(g)} = S_{t1} \mu t_{x_3}^{(g)} \tag{9}$$

$$t_{x_2}^{(g)} = S_{t2} \mu t_{x_3}^{(g)} \tag{10}$$

where  $\delta$  is an initial gap possibly between the contact nodes and  $\mu$  is the coefficient of contact friction.  $S_{t1}$  and  $S_{t2}$  are equal to +1 or -1 if the slip occurs along or opposite the directions of the  $x_1^{(g)}$  and  $x_2^{(g)}$  axes, respectively.

### **2.4 Coupling the system equations**

Eq. 1 for the indenter and Eq. 2 for the FGM are then coupled together at the contact nodes. Two sets of simultaneous linear equation systems can be expressed in matrix form as follows:

$$\begin{bmatrix} \mathbf{A}^{(g)} & \mathbf{0} \\ \mathbf{0} & \mathbf{A}^{(m)} \end{bmatrix} \begin{bmatrix} \mathbf{u}^{(g)} \\ \mathbf{u}^{(m)} \end{bmatrix} = \begin{bmatrix} \mathbf{B}^{(g)} & \mathbf{0} \\ \mathbf{0} & \mathbf{B}^{(m)} \end{bmatrix} \begin{bmatrix} \mathbf{t}^{(g)} \\ \mathbf{t}^{(m)} \end{bmatrix} \tag{11}$$

where  $\mathbf{u}$  and  $\mathbf{t}$  are the sub-matrices of the displacement and tractions, respectively; the sub-matrices  $\mathbf{A}$  and  $\mathbf{B}$  are the coefficient matrices of the displacements and tractions, respectively.

Eq.11 can be re-written in terms of sub-matrices for the global directions for all nodes. Eq.11 is further converted from the global coordinate expressions to the local coordinate expressions. Subsequently, the contact equations in Eqs. 3 to 10 can be incorporated into Eq.11.

For the first contact case, the BEM results can be directly obtained by solving the new linear equations. However, for the second contact case, it is necessary to solve a series of the linear equations in an iterative process until all the other conditions are met. These conditions include that there are not tensile stresses in contact area and no overlap outside the contact area. The frictional slipping or sticking is judged in the iterative process.

### **2.5 Displacements and stresses in FGM**

After having obtained the contact displacements and three contact stresses, the displacements and stresses at any point within FGM can be further obtained with the following expressions

$$\begin{aligned} u_i(q) &= \int_{S_2} u_{ij}^Y(q, P) t_j(P) dS(P) \\ \sigma_{ij}(q) &= \int_{S_2} \sigma_{ijk}^Y(q, P) t_k(P) dS(P) \end{aligned} \tag{12}$$

where  $u_{ij}^Y$  and  $\sigma_{ijk}^Y$  are the displacements and stresses at the  $q$  point induced by  $t_j$  (or  $t_k$ ) located at the  $P$  point in the FGM.

It is noted that Eq.12 has the integrals of weak and strong singularities for computing the additional displacements and stresses on the contact surface. So, Eq.12 is not used for the values at the contact surface. Instead, the results at the nodes and the constitutive equations are used for accurate values of the displacements and stresses at any point on the contact surface (Brebbia et al. 1984).

### 3 Numerical verifications

#### 3.1 Numerical verification A

Two conventional contact problems are used for the numerical verifications. The first is the normal contact of circular elastic cylinder on a homogeneous elastic solid of semi-infinite extent. The cylinder has a unit radius  $a$  ( $= 1$ ), height  $2a$ , elastic modulus  $E_p$  and Poisson's ratio 0.2. Its upper flat surface is subjected to a uniform pressure  $p_0$ . Its lower flat surface fully contacts with the elastic foundation.

Due to symmetry, a quarter of the cylinder and foundation system is discretized. The boundary element meshes are shown in Fig. 2. The contact surface has 76 eight-noded elements. The cylinder has 232 eight-noded elements.

The exact solution for a smooth rigid cylinder is available in the literature. The non-dimensional rigid cylinder settlement can be expressed as follows.

$$W = w_0 a E_f / p_0 (1 - \nu^2) = 0.3184 \quad (13)$$

where  $E_f$  and  $\nu$  are respectively the elastic modulus and Poisson's ratio of the foundation, and  $w_0$  is the rigid cylinder settlement.

The non-zero contact stress is the normal stress and expressed as follows:

$$p(r) = p_0 / \left( 2\sqrt{1 - r^2} \right) \quad (14)$$

where  $r(0 \leq r < 1)$  is the radial distance.

The BEM results for the non-dimensional rigid cylinder settlement  $W$  at the contact center are 0.3153 and 0.3137 for  $E_p/E_f = 10^2$  and  $E_p/E_f = 10^5$ , respectively, which are close to the rigid cylinder value 0.3184. The BEM results for the non-zero normal contact stress are shown in Fig. 3, where  $E_p/E_f = 1, 10, 10^2$  and  $10^5$ , respectively. It is evident that as  $E_p/E_f$  increases, the normal contact stress becomes closer and closer to the exact solution.

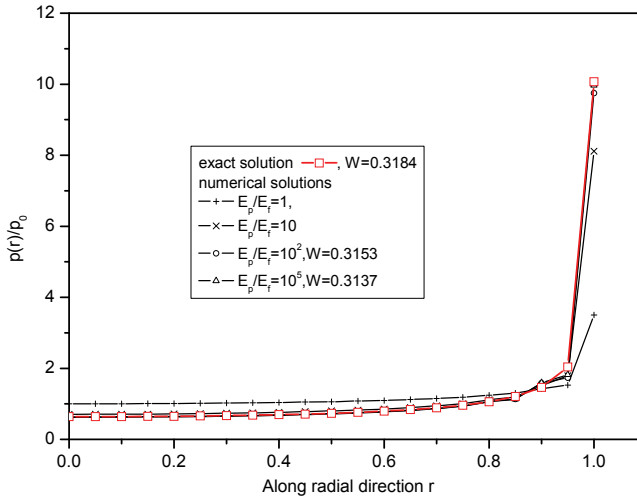


Figure 3: Axisymmetric normal contact stresses for different modulus ratios between the cylinder and the base

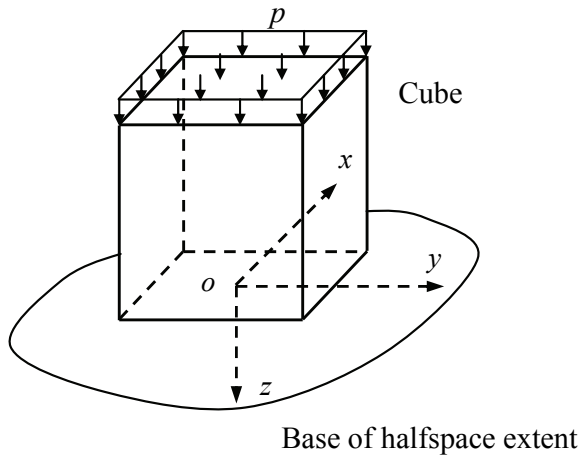


Figure 4: Normal indentation of a cube on homogeneous elastic base of half space

### 3.2 Numerical verification B

The second is the indentation of an elastic cube on a homogeneous elastic base of half space extent, as shown in Fig. 4. The cube has a side length 2.0 m and has the same elastic constants as the elastic base. The elastic modulus is  $E$  and the

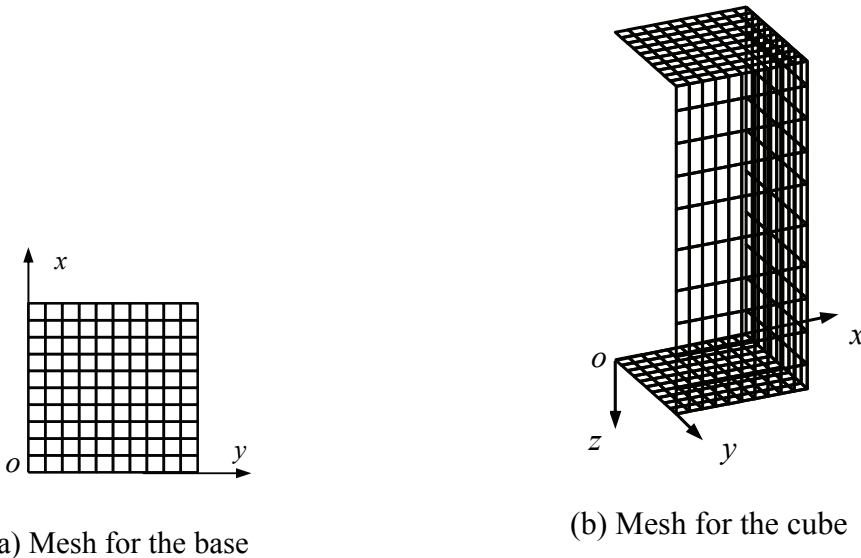


Figure 5: FEM meshes for normal indentation of a cube on homogeneous elastic base of half space

Poisson's ratio  $\nu = 0.2$ . The friction coefficient  $\mu = 0$  or  $\mu = 0.2$  is used for the contact surface. The uniform pressure  $p$  has the same value as the elastic modulus  $E$ . The BEM meshes are shown in Fig. 5. Due to symmetry, a quarter of the cube and the base system is discretized. The contact surface has 100 eight-noded elements (Fig. 5a). The cube has 400 eight-noded elements (Fig. 5b). It is noted that a similar contact problem was considered in Leathy and Becker (1999b), where the base was limited to a rectangular solid of height 4 m, width 16 m and depth 16 m.

The present BEM results for the normal and shear stresses are shown in Figs. 6 and 7, respectively, where the FEM and BEM results in Leathy and Becker (1999b) are also plotted. The normal contact stress values from the present study have a good agreement with the results in Leathy and Becker (1999b). However, the shear contact stress values have some differences with the results in Leathy and Becker (1999b). Furthermore, the normal contact stress within the inner contact region is slightly lower for the frictional contact  $\mu = 0.2$  than for the smooth contact  $\mu = 0.0$ .

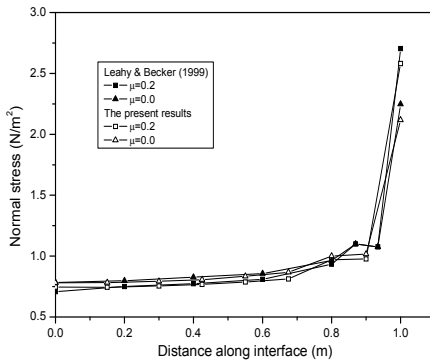


Figure 6: Normal contact stress results and comparison with others' results

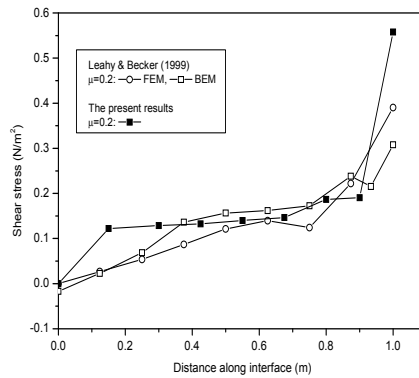


Figure 7: Shear contact stress results and comparison with others' results

## 4 Applications

### 4.1 The FGM contact problem

Fig. 8 illustrates the FGM contact problem examined in this study. The elastic rectangular plate is subject to a point normal load  $P_z$  (3000 N) and is in smooth contact with the FGM. The plate is 2 mm long, 1 mm wide and 0.25 mm high. Accordingly, the contact area is 2 mm by 1 mm. The plate has its elastic modulus  $E_p=10^{10}$  GPa. So, it is rigid.

The graded material of  $\text{Si}_3\text{N}_4$ -based ceramics in Pender et al. (2001) is used as the FGM. The FGM has a constant Poisson's ratio 0.22 and a depth variable elastic modulus (GPa) as follows.

$$\begin{aligned}
 E(z) &= 225.01 + 370.6z, & 0 \leq z \leq 0.05\text{mm} \\
 E(z) &= 243.54 + 76.4(z - 0.05), & 0.05 \leq z \leq 0.10\text{mm} \\
 E(z) &= 247.36 + 450.8(z - 0.1), & 0.10 \leq z \leq 0.15\text{mm} \\
 E(z) &= 269.90 + 145.0(z - 0.15), & 0.15 \leq z \leq 0.20\text{mm} \\
 E(z) &= 277.20 + 122.2(z - 0.20), & 0.20 \leq z \leq 0.25\text{mm} \\
 E(z) &= 283.26 - 53.4(z - 0.25), & 0.25 \leq z \leq 0.30\text{mm} \\
 E(z) &= 280.59 + 294.1(z - 0.30), & 0.30 \leq z \leq 0.40\text{mm} \\
 E(z) &= 310.0, & z \geq 0.40\text{mm}
 \end{aligned} \tag{15}$$

where  $z$  is the depth as shown in Figs. 8 and 9.

The FGM from the depth 0 to 0.4 mm is discretized into 30 thin layers, as shown in Fig. 9. Each layer has a constant modulus from Eq. 9. The FGM from the depth 0.4 mm to  $\infty$  is modeled as a homogeneous elastic solid of lower halfspace extent.

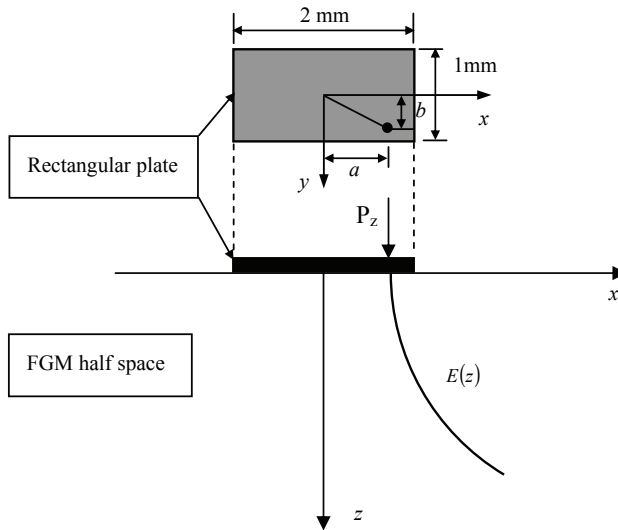


Figure 8: Eccentric indentation of an elastic rectangular plate on FGM halfspace

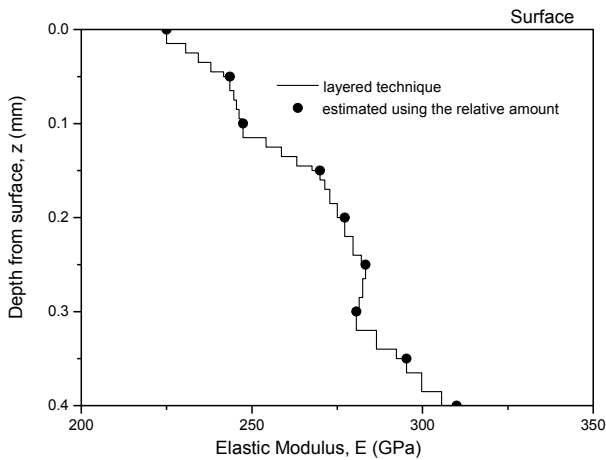


Figure 9: Arbitrary variation of elastic modulus in layer for actual measured modulus

For comparison, the FGM is also modeled as a homogeneous elastic solid of lower halfspace extent. Its elastic modulus is equal either to the lower limit 225.01 GPa at  $z = 0$  or the upper limit 310 GPa at  $z = 0.4$  mm of the actual FGM.

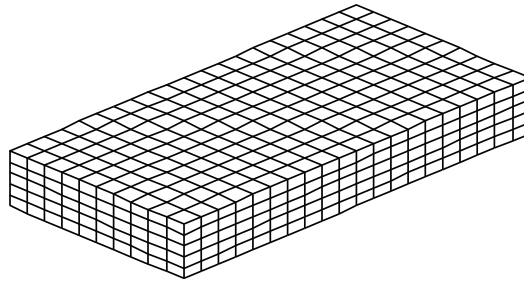


Figure 10: BEM mesh of 724 elements and 2122 nodes for the elastic rectangular plate with high modulus

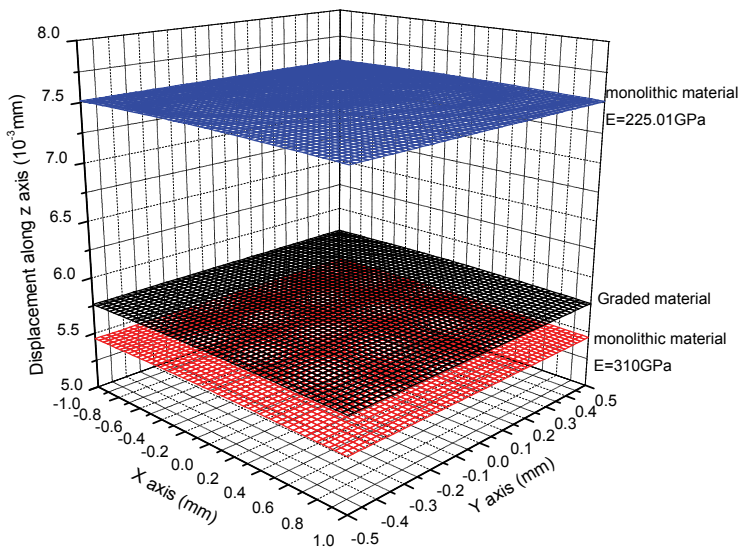


Figure 11: Vertical displacements of the contact surface due to central load

The point normal load  $P_z$  is applied at either the plate centre (0, 0, -0.25 mm) or an eccentric point (0.6 mm, 0.3 mm, -0.25 mm) above the plate. The BEM mesh for the plate is shown in Fig. 10. The contact surface has 200 elements and 661 nodes.

**4.2 BEM results for the central load application**

Fig. 11 shows the vertical displacements of the contact surface for the three FGM modulus cases: the lower limit, the actual FGM and the upper limit. The results are

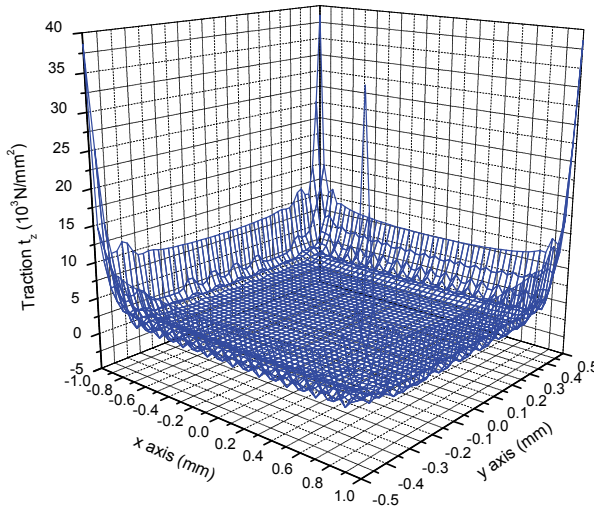


Figure 12: Normal contact stress of actual FGM under the central load

expected since the vertical displacement for the actual FGM is  $6.47 \times 10^{-3}$  mm and is bounded by  $7.51 \times 10^{-3}$  mm and  $5.45 \times 10^{-3}$  mm for the lower and upper limit modulus cases, respectively.

Fig. 12 shows the normal contact stress for the actual FGM. As expected, the normal contact stress has high concentrations along the contact circumference. Fig. 13 further shows the normal contact stresses for the actual FGM and its two limits along the  $x$ -axis. The contact stress values for the two limit cases are almost identical but higher than those of the actual FGM.

Fig. 14 shows the distributions of the vertical normal stresses at the two depths ( $z = 0.032$  mm or  $0.07$  mm) along the  $x$ -axis under the central load. Fig. 15 further shows the vertical normal stresses at the two depths ( $z = 0.032$  mm or  $0.07$  mm) along the  $x$ -axis with an offset  $y = 0.5$  mm under the central load. As the depth  $z$  increases, the normal stress concentrations near the contact circumference become less and less. In addition, the FGM results in limited change in the vertical normal stress in comparison with the homogeneous elastic solids (i.e., the two limit cases).

### 4.3 BEM results for the eccentric load application

Fig. 16 shows the vertical displacements of the contact surface for the three FGM modulus cases. As expected, the vertical displacement for the actual FGM is bounded by those for the lower and upper limit modulus cases, respectively. In

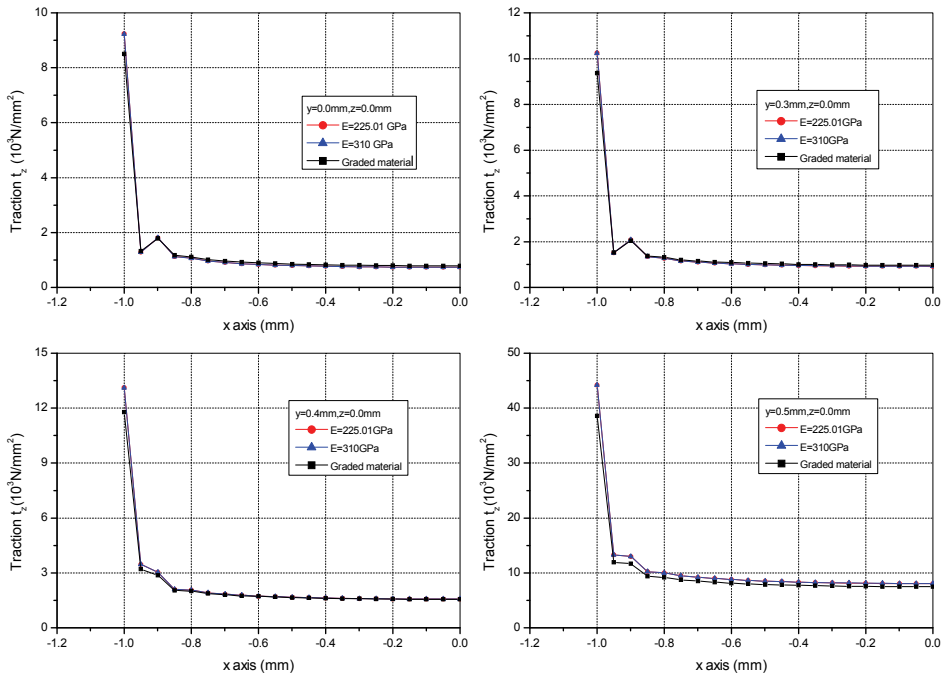


Figure 13: Normal contact stresses of the actual FGM and its two limits along the  $x$ -axis with different offsets  $y = 0.0, 0.3, 0.4$  or  $0.5$  mm under the central load

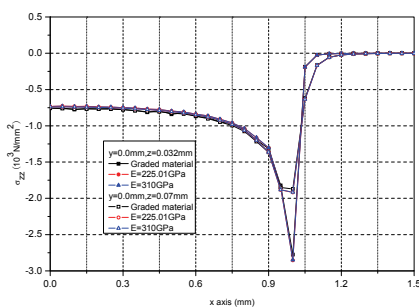


Figure 14: Vertical normal stresses  $\sigma_{zz}$  at the depth  $z = 0.032$  or  $0.07$  mm along the  $x$ -axis under the central load

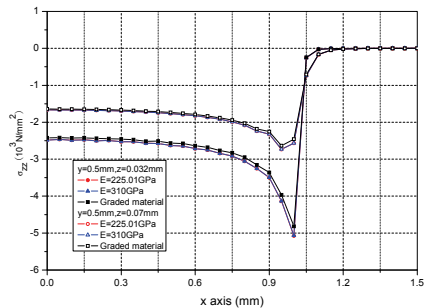


Figure 15: Vertical normal stresses  $\sigma_{zz}$  at the depth  $z = 0.032$  or  $0.07$  mm along the  $x$ -axis with an offset  $y = 0.5$  mm under the central load

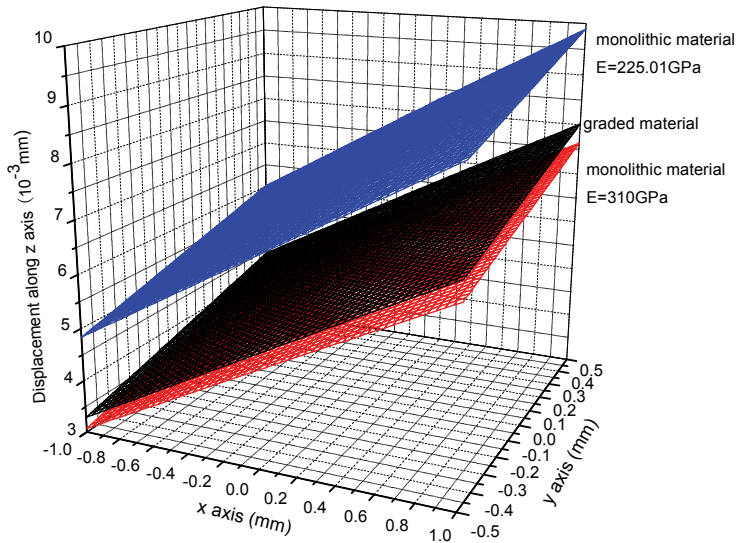


Figure 16: Vertical displacements of the contact surface due to the eccentric load

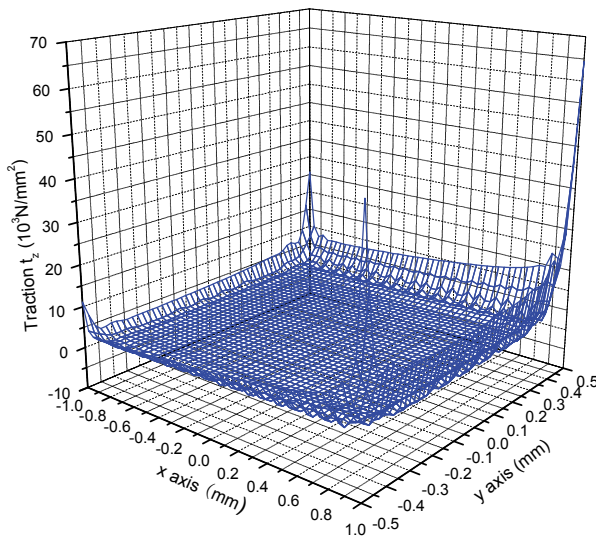


Figure 17: Normal contact stress of actual FGM under the eccentric load

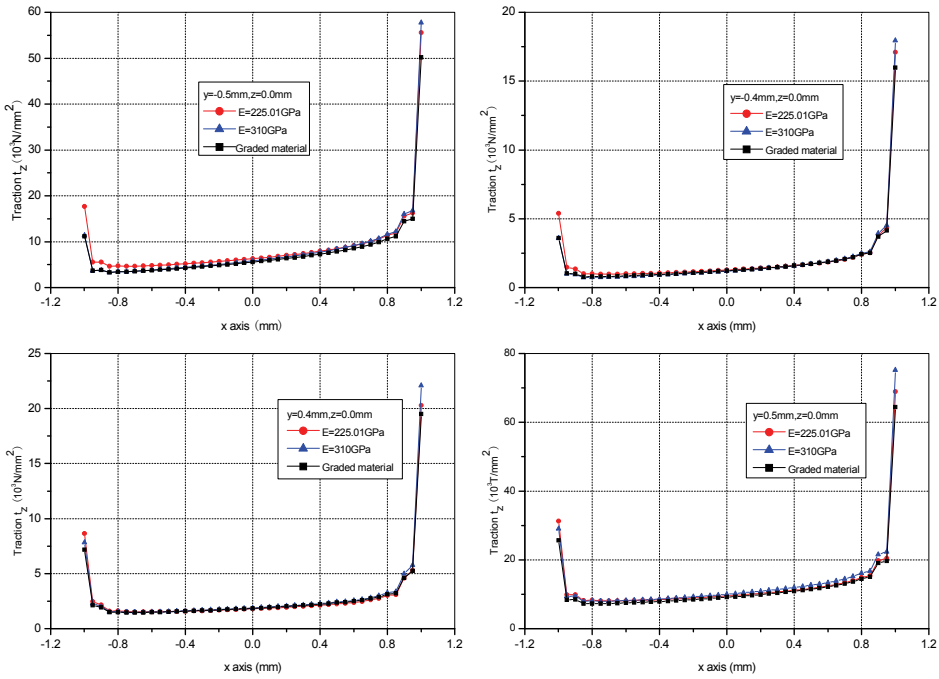


Figure 18: Normal contact stresses of the actual FGM and its two limits along the  $x$ -axis with different offsets  $y = -0.5, -0.4, 0.4$  or  $0.5$  mm under the eccentric load

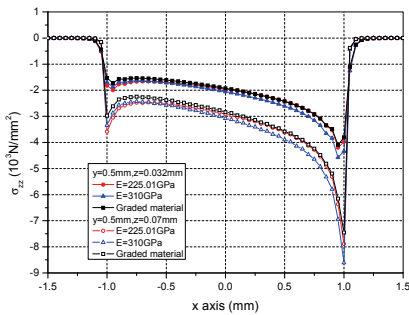


Figure 19: Vertical normal stresses at the depth  $z = 0.032$  or  $0.07$  mm along the  $x$ -axis with an offset  $y = 0.5$  mm under the eccentric load

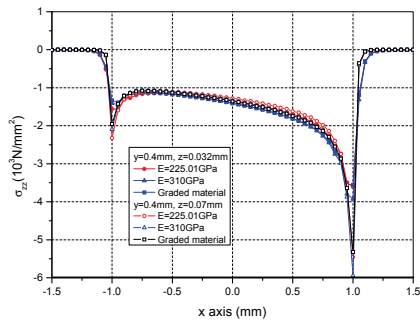


Figure 20: Vertical normal stresses at the depth  $z = 0.032$  or  $0.07$  mm along the  $x$ -axis with an offset  $y = 0.4$  mm under the eccentric load

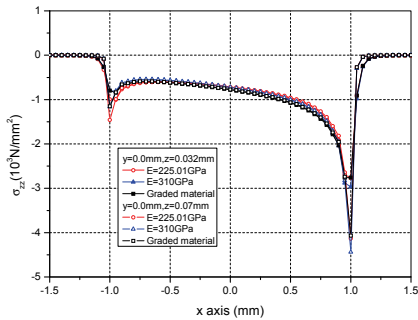


Figure 21: Vertical normal stresses at the depth  $z = 0.032$  or  $0.07$  mm along the  $x$ -axis under the eccentric load

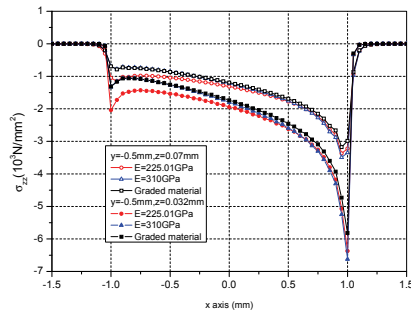


Figure 22: Vertical normal stresses at the depth  $z = 0.032$  or  $0.07$  mm along the  $x$ -axis with an offset  $y = -0.5$  mm under the eccentric load

addition, the maximum vertical displacements are at the corner point  $(1.0, 0.5, 0.0)$  and the minimum vertical displacements are at the corner point  $(-1.0, -0.5, 0.0)$  for the three cases. The eccentric load does not cause any tension or gap between the plate and its elastic base.

Fig. 17 shows the distribution of the normal contact stress associated with the actual FGM under the eccentric load. The normal contact stress has concentrations along the plate circumference. Its highest is located at the corner  $(1.0, 0.5, 0.0)$  and the lowest at the corner point  $(-1.0, -0.5, 0.0)$ , which correspond to the locations of the maximum and minimum vertical displacements. Its second and third high values are located at the third and fourth corners  $(1.0, -0.5, 0.0)$  and  $(-1.0, 0.5, 0.0)$ , respectively.

Fig. 18 shows a comparison among the normal contact stresses for the actual FGM and its two limit cases along the  $x$ -axis with different offsets  $y = 0.0, 0.3, 0.4$  or  $0.5$  mm, respectively. At the edge  $x = 1.0$  mm, the values of the normal contact stress are the highest, the intermediate and the smallest for the upper limit case, the lower limit case and the FGM case, respectively. However, at the opposite edge  $x = -1.0$  mm, the value of the normal contact stress for the lower limit case is the highest.

Figs. 19-22 show the distribution of the vertical normal stress for the three cases at the two depths ( $z = 0.032$  mm or  $0.07$  mm) along the  $x$ -axis with offsets of  $y = 0.5, 0.4, 0.0$  and  $-0.5$  mm, respectively. The highest values of the vertical normal stress are located at the edge  $x = 1.0$  mm. The vertical normal stresses also have the local peaks at the edge  $x = -1.0$  mm. As the depth  $z$  increases, the normal stress concentrations near the contact circumference become less and less. In addition, the FGM results in noticeable changes in the vertical normal stress in comparison

with the homogeneous elastic solids (i.e., the two limit cases).

## 5 Conclusions

This paper presents a generalized Kelvin solution based BEM for the analysis of the normal indentation of an elastic cylinder on a FGM. The numerical verifications show that the proposed method can obtain the satisfactory results for the contact problems. In particular, the method is applied to the contact problem of an elastic indenter on a FGM base. The BEM results have shown that the FGM has some effects on the contact displacement and contact stress and the vertical normal stress field in the elastic base solid.

**Acknowledgement:** The authors would like to thank the financial supports from The Special Fund of Tai Shan Scholars of Shandong Province and the University of Hong Kong. The authors would also like to thank the peer reviewers and the corresponding editor, Professor A.P.S. Selvadurai, for their valuable comments and suggestions.

## References

- Blázquez, A.; París, F.** (2009): On the necessity of non-conforming algorithms for ‘small displacement’ contact problems and conforming discretizations by BEM, *Engineering Analysis with Boundary Elements*, vol. 33, pp. 184-190.
- Booker, J.R.; Balaam, N.P.; Davis, E.H.** (1985): The behaviour of an elastic non-homogeneous halfspace: Part II, *International Journal for Numerical and Analytical Methods in Geomechanics*, vol.9, pp.369-381.
- Brebbia, C.A.; Telles, J.C.F.; Wrobel, L.C.** (1984): *Boundary element techniques*, Computational Mechanics Publications, Southampton.
- Gladwell, G.M.** (1980): *Contact problems in the classical theory of elasticity*, Kluwer Academic Publishers, Dordrecht.
- Guler, M.A.; Erdogan, F.** (2006): Contact mechanics of two deformable elastic solids with graded coatings, *Mechanics of Materials*, vol.38, pp.633–647.
- Gun, H.** (2004): Boundary element analysis of 3D elastic-plastic contact problems with friction, *Computers and Structures*, vol.82, pp.555-566.
- Hack, R.S.; Becker, A.A.** (1999): Frictional contact analysis under tangential loading using a local axes boundary element formulation, *International Journal of Mechanical Sciences*, vol.41, pp.419-436.
- Hills, D. A.; Nowell, D.; Sackfield, A.** (1993): *Mechanics of elastic contacts*, Butterworth, Heinemann, Oxford.

**Leahy, J.G.; Becker, A.A.** (1999a): A quadratic boundary element formulation for three-dimensional contact problems with friction, *Journal of Strain Analysis*, vol.34, pp.235-251.

**Leahy, J.G.; Becker, A.A.** (1999b): The numerical treatment of local variables in three-dimensional frictional contact problems using the BEM, *Computers and Structures*, vol.71, pp.383-395.

**Johnson, K.L.** (1985): *Contact mechanics*, Cambridge University.

**Keppas, L.K.; Giannopoulos, G.I.; Anifantis, N.K.** (2008): Transient coupled thermoelastic contact problems incorporating thermal resistance: a BEM approach, *CMES: Computer Modeling in Engineering & Sciences*, vol. 25, pp.181-196.

**Man, K.W.; Aliabadi, M.H.; Rooke, D.P.** (1993): BEM frictional contact analysis: load incremental techniques, *Computers and Structures*, vol.47, pp.893-905.

**Oishi, A.; Yoshimura, S.** (2008): Genetic approaches to iteration-free local contact search, *CMES: Computer Modeling in Engineering & Sciences*, vol. 28, pp. 127-146.

**Olukoko, O.A.; Becker, A.A.; Fenner, R.T.** (1994): A review of three alternative approaches to modeling frictional contact problems using the BEM, *Proceedings of the Royal Society London A*, vol.444, pp.37-51.

**Pak, R.Y.S.; Simmons, B.M.; Ashlock, J.C.** (2008): Tensionless contact of a flexible plate and annulus with a smooth half-space under axisymmetric loads by integral equations, *International Journal of Mechanical Sciences*, vol.50, pp.1004-1011.

**Pender, D.C.; Padture, N.P.; et al.** (2001): Gradients in elastic modulus for improved contact-damage resistance: Part I, *Acta Materialia*, vol.49, pp.3255-3262.

**Rajapakse, R.K.N.D.; Selvadurai, A.P.S.** (1991): Response of circular footings and anchor plates in non-homogeneous elastic soils. *International Journal for Numerical and Analytical Methods in Geomechanics*, vol.15, pp.457-470.

**Rowe, R.K.; Booker, J.R.** (1981): The behaviour of footings resting on a non-homogeneous soil mass with a crust: Part II, *Canadian Geotechnical Journal*, vol.18, pp.265-279.

**Selvadurai, A.P.S.** (1979): *Elastic Analysis of Soil-foundation Interaction. Developments in Geotechnical Engineering*, vol.17, Elsevier Scientific, Amsterdam, The Netherlands.

**Selvadurai, A.P.S.** (1996): The settlement of a rigid circular foundation resting on a halfspace exhibiting a near surface elastic non-homogeneity, *International Journal for Numerical and Analytical Methods in Geomechanics*, vol. 20, pp.351-364.

**Selvadurai, A.P.S.** (2007): The analytical method in geomechanics, *Applied Mechanics Reviews*, vol. 60, pp. 87-106.

**Vignjevic, R.; Vuyst, T. D.; Campbell, J.C.** (2006): A frictionless contact algorithm for meshless methods, *CMES: Computer Modeling in Engineering & Sciences*, vol.13, pp. 35-48.

**Xiao, H.T.; Yue, Z.Q.; Tham, L.G.** (2005): Analysis of an elliptical crack parallel to graded interfacial zone of bonded bi-materials. *Mechanics of Materials*, vol.37, pp.785-799.

**Yue, Z.Q.** (1995): On generalized Kelvin solutions in a multilayered elastic medium. *Journal of Elasticity*, vol.40, pp.1-43.

**Yue, Z.Q.** (1996): Elastic field for eccentrically loaded rigid plate on multilayered solids. *International Journal of Solids and Structures*, vol.33, pp.4019-4049.

**Yue, Z.Q.; Selvadurai, A.P.S.** (1995): Contact problems for saturated poroelastic solid, *Journal of Engineering Mechanics*, vol. 121, pp.502-512.

**Yue, Z.Q.; Xiao, H.T.** (2002): Generalized Kelvin solution based boundary element method for crack problems in multilayered solids, *Engineering Analysis with Boundary Elements*, vol.26, pp.691-705.

**Yue, Z.Q.; Yin, J.H.; Zhang, S.Y.** (1999): Computation of point load solutions for geo-materials exhibiting elastic non-homogeneity with depth, *Computers and Geotechnics*, vol.25, pp.75-105.

